

**REGIONAL GEOLOGY OF THE CHANG'E-3 LANDING ZONE II.** Y. Z. Wu<sup>1</sup>, J. W. Head<sup>2</sup>, C. M. Pieters<sup>2</sup>, A. T. Basilevsky<sup>3</sup>, L. Li<sup>4</sup>. <sup>1</sup>School of Geographic and Oceanographic Sciences, Nanjing University, Nanjing, 210023, China (wu@nju.edu.cn), <sup>2</sup>Dept. Earth, Environmental and Planetary Sciences, Brown University, Providence, RI 02912 USA, <sup>3</sup>Vernadsky Institute of Geochemistry and Analytical Chemistry Russian Academy of Sciences, Moscow, Russia. <sup>4</sup>Department of Earth Sciences, Indiana University-Purdue University, Indianapolis, IN 46202 USA.

**Introduction:** On the basis of our previous trilateral (Russia-China-USA) research [1] in the composition and geologic context of the Chang'E-3 (CE-3) landing zone and the surroundings, we conducted further investigation of the Mare Imbrium/Imbrium basin region. The goal of this trilateral analysis is to provide a regional context for the history of the Imbrium basin, and to document the nature and evolution of the geologic units that they contain. This detailed analysis will help to interpret the *in situ* data acquired by the CE-3 rover and provide important input into future planning for optimizing lunar surface mission payloads, traverse planning and operations, and returned sample missions.

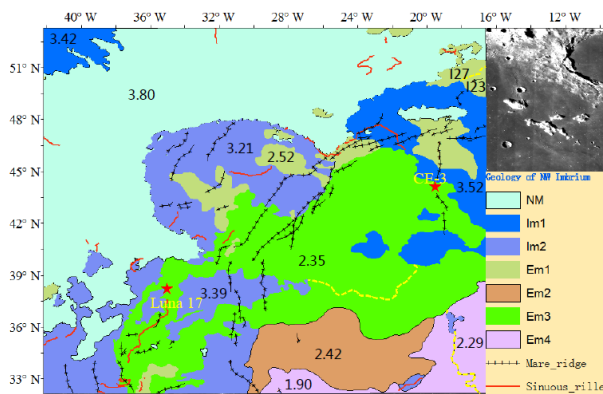


Fig. 1. Geologic map of the northwest Imbrium. The highlands are named with NM (non-mare materials) to distinguish farside highlands.

**Materials and Methods:** A variety of orbital remote sensing data was used in this study. The abundances of elements were derived from Gamma ray spectroscopy [2]. The mineralogy was inferred from data from the Moon Mineralogy Mapper ( $M^3$ ) onboard Chandrayaan-1. The Chang'E-1 Interference Imaging Spectrometer (IIM) data were used as the base map for the division of spectral units and the Lunar Reconnaissance Orbiter Camera (LROC) Wide Angle Camera (WAC) data were used for measuring crater size-frequency distributions (CSFDs), which aimed to derive absolute ages.

#### Regional Geology and Spectral Geologic Map:

The research area (Fig. 1) lies in the northwest Procellarum-KREEP Terrain (PKT) [3] and its geology is dominated by the formation of the Imbrium basin. Fig. 1 shows a new geologic map resulting from integration of various remote sensing data. Iridium, a probable peaking basin based on its size ( $D \sim 236$  km), was formed at 3.8 Ga and heavily modified the rim/ring structure of

NW Imbrium basin. The ages of the exposed basalts span a large range from the Imbrian to late Eratosthenian Period. The Eratosthenian basalts were classified into four units (Em1-Em4, older to younger). The oldest Eratosthenian unit, Em1, is  $\sim 2.52$  Ga. The CE-3 landing site unit,  $\sim 2.35$  Ga, belongs to Em3.

Abundant linear and curvilinear structures (sinuous rilles, mare ridges, rupes and catenae) exist in this area. Linear troughs interpreted to be graben, however, are not apparent. The strikes of the sinuous rilles in the highlands are serpentine and controlled by the topography indicating volcanic origin. They spread around Sinus Iridium. The fracture in the highlands caused by the Iridium impact may provide possible channels for the upwelling of magma, which formed sinuous rilles. The sinuous rilles in the maria are also widespread. The sinuous rilles or possible lava channels in the Eratosthenian basalts are well-preserved and very narrow indicating weak magmatism in the late stage of the Moon. Seven very narrow rilles were identified using the  $M^3$  thermal bands. They lacked an associated source depression, except the shortest rill ( $\sim 2.8$  km,  $33.00^\circ$ ,  $-36.34^\circ$ ) has a plausible source depression. Wrinkle ridges are widely distributed in Sinus Iridium and Mare Imbrium. Many mare ridges are concentric to the Imbrium Basin suggesting that they are influenced by basin structures. The CE-3 lunar module was on one NW linear ridge which was buried by the Em3 basalt and at the transition zone of the positive and negative free-air gravity anomaly [4].

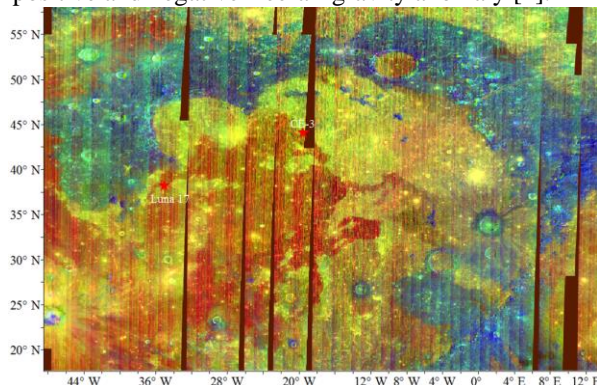


Fig. 2. The  $M^3$  integrated band depth (IBD) color composite (R-1  $\mu\text{m}$  BID, G-2  $\mu\text{m}$  BID, B- reflectance at 1.58  $\mu\text{m}$ ). Blue indicates lack of absorption. Cyan is representative of norite or noritic anorthosite and purple is representative of dunite or troctolite, both of which are readily identified in the highlands in a higher resolution version of the figure. Greenish yellow is representative of pyroxene-rich mare basalts, and the red is representative of olivine-rich basalts.

**Mafic-rich Compositions in the Highlands:** Compared to the farside highlands, the highlands surrounding Imbrium exhibit abundant mafic-rich areas indicated by  $M^3$  integrated band depth composite (IBD, Fig. 2) and elevated concentrations of Fe and Th [2]. The FeO abundance ranges from 8 to 15 wt.% with an average of  $\sim 12.8$  wt.%. The spectra from fresh craters indicate that Mg-rich pyroxenes and olivine-bearing rocks (Figs. 3 & 4) are common here rather than anorthosite, which dominates the farside highlands. The mafic minerals and elevated FeO indicate that a huge impact has removed much of the feldspathic lunar crust and exposed the lower mafic-rich crust. This supports the opinion of [5] that the lunar crust become more mafic, noritic composition with depth.

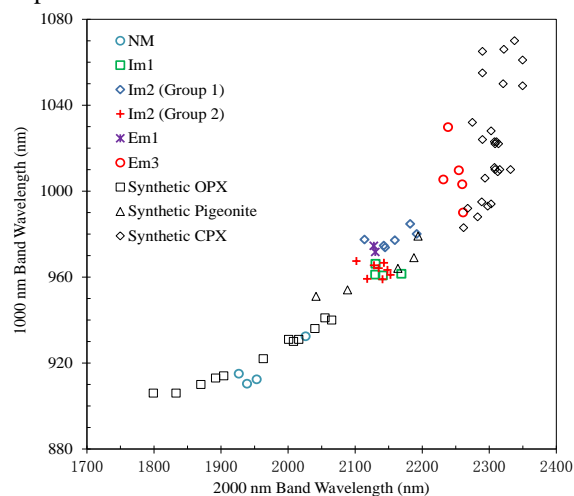


Fig. 3. Comparison of the 1  $\mu\text{m}$  vs 2  $\mu\text{m}$  band positions for fresh craters of highlands and mare basalts with synthetic pyroxenes [6].

**Mineralogy of Mare Basalts:** A scatter plot of 1 vs 2  $\mu\text{m}$  band positions for the basaltic units of the research area and synthetic pyroxenes is shown in Fig. 3. The most obvious feature is that the Eratosthenian Hi-Ti basalts fall above the pyroxene trend. A similar trend was also found for the Eratosthenian Hi-Ti basalts in Oceanus Procellarum [7]. The spectra of the three young Eratosthenian units (Ems 2-4) exhibit longer center of wide 1  $\mu\text{m}$  absorption, strong 1.3  $\mu\text{m}$  absorption and very weak 2  $\mu\text{m}$  absorption, consistent with olivine-rich basalts (Fig. 4). The oldest unit of the study area, Im1 (the underlying unit of CE-3 site), has uniform features with shorter band centers, indicating less Fe or Ca in pyroxene. The Im2 unit, mostly developed in the west, is more compositionally diverse and can be divided into two groups. The two groups spatially overlap, which makes it difficult to separate geologic units based on spectral parameters. Group 1 exhibits 1  $\mu\text{m}$  absorption in wavelengths slightly longer than Group 2 (Fig. 3) possibly indicating more olivine, which is consistent with its weaker 2  $\mu\text{m}$  band but strong 1.3  $\mu\text{m}$  absorption. Group

2 overlaps with Im1, however, its 1.3  $\mu\text{m}$  absorption is weaker than Im1.

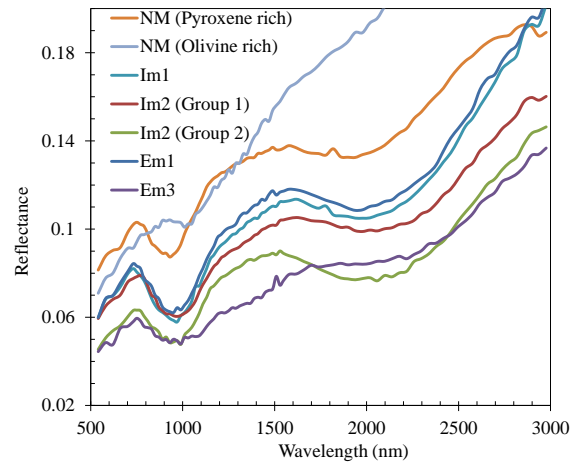


Fig. 4. Example spectra of fresh craters from geologic units corresponding to Fig. 3.

**Thickness and Flux of Em3 Unit:** Figure 5 shows the thickness map of Em3, which was derived in terms of the distinct difference of the spectra between Em3 and its underlying unit [8]. The thickness of Em3 ranges from  $\sim 15$  m to  $\sim 50$  m, consistent with the results of [9, 10]. The Em3 unit has an estimated volume of  $\sim 3.387 \times 10^3$   $\text{km}^3$  and estimated average eruption flux of 48  $\text{km}^3/\text{Ma}$ . This flux, plus the simultaneous basalts with similar compositions emplaced in the Oceanus Procellarum suggests that the late stage basalts could be more extensive than previously thought [11].

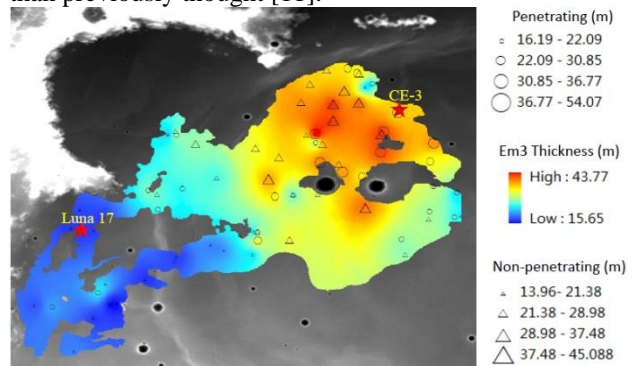


Fig. 5. Raster map of the estimated thickness of the Em3 basalts.

**References:** [1] Wu Y. Z. et al. (2014) *LSPC*, Abstract #2613. [2] Prettyman T. H. (2006) *JGR*, 111, E12007. [3] Jolliff B. L. et al. (2000) *JGR*, 105, E2,4197-4216. [4] Xu Y. B. et al. (2012) *Earth Science Frontiers*, 19(6), 60-71. [5] Pieters C. M. et al. (2013) *LSPC XLIV*, Abstract #2545. [6] Klima R. L. et al. (2011) *JGR*, 116(E6). [7] Staid M. I. et al. (2011) *JGR*, 116, E00G10, doi:10.1029/2010JE003735. [8] Chen Y. et al. (2015) *LPS XLVI*, this conference. [9] Zhao J. N. et al. (2014) *Sci China-Phys Mech Astron.* 1-8. [10] Qiao L. et al. (2014) *PSS*, 101, 37-52. [11] Head J. W. et al. (1992) *GCA*, 56(6), 2155-2175.